BEAM-RESIDUAL GAS INTERACTIONS

Søren Pape Møller
ISA, Aarhus University, Denmark

Abstract

The interactions between a beam of charged particles and the residual gas will be described. In principle we should cover beams consisting of any type of charged particles. Clearly, this is an impossible task, but most types are included. Also, only the most important interactions are described. The interactions between the beam and the residual gas will lead to a reduction in the lifetime, and possibly an increase of the beam emittance. Knowing the cross section for the interaction in question, these effects can be calculated. Finally, the effects these interactions will have on the surroundings in terms of radiation and background will be mentioned briefly.

1. INTRODUCTION

The performance of accelerators and storage rings depends on the many components of the accelerator, and one very important component is the vacuum system. Interactions between the accelerated particles and the residual-gas atoms may degrade the beam quality. The lifetime may be reduced and/or the emittance may increase. Ideally, the aim is to obtain an average pressure so low, that the effects from the beam-residual gas interactions may be neglected altogether in comparison with other effects, for example beam-beam effects. A finite pressure can also lead to losses in transfer beam lines, but the requirements to the pressure in such beam lines are usually much more relaxed than in cyclic accelerators.

I will describe the interactions between the beam particles and the residual-gas atoms/molecules in general terms, and try to include most species. Hence both negative ions, positive ions of both low- and high-charge states, and both molecular and atomic ions are considered. Furthermore, electrons and positrons will be included. The energy range will be very wide, starting from very low energies of the order of keV and ending at very high energies in the multi-GeV region.

Emphasis is given to the physical principles, and although some exact formulae are given, crude estimates are often sufficient in order to evaluate the pressure required. Most of the vacuum related effects have been described in proceedings from previous CERN accelerator schools. Concerning electrons and positrons, see Refs. [1, 2], and for ions see [3]. As a slight addition to these treatments, the present description is more unified and formulae apply to both light and heavy projectiles.

2. THE CONCEPTS OF CROSS SECTIONS AND LIFETIMES

Consider a beam of intensity I, that is I particles per cm^2 per second, crossing a target of thickness dx with density n atoms per cm^3. This beam will now be attenuated by the collisions, and the change in intensity dI will be proportional to I, n and dx

$$dI = -I\sigma n dx$$

where the constant of proportionality σ has the dimensions of an area and is called the cross section. The cross section can be interpreted as the area of the atom inside which the considered reaction will take place; see Fig. 1. First estimates of the cross sections for the relevant processes are geometrical cross sections, which for atomic and nuclear processes would correspond to $\sigma = \pi r^2 \approx \pi(1 \text{ Å})^2 = 3 \cdot 10^{-16} \text{cm}^2$ and $\sigma = \pi r^2 \approx \pi(10 \text{ fm})^2 = 3 \cdot 10^{-24} \text{ cm}^2$, respectively. So it is immediately seen that nuclear processes can often be neglected in comparison with atomic ones. We shall later return to more accurate estimates.

The target thickness traversed is given by $dx = vdt = \beta cdt$, where v and c are the velocities of the projectiles and the speed of light, respectively. The solution to the above equation is then

$$I = I_0 \exp(-t/\tau).$$

Hence the intensity will decay exponentially, with a lifetime τ given by

$$\tau = \frac{1}{v\sigma n} \quad .$$

When there are more processes of comparable significance, the cross sections should be added $\sigma_{\text{total}} = \sigma_1 + \sigma_2 + ..$, or the inverse lifetimes, the decay rates, should be added $1/\tau_{\text{total}} = 1/\tau_1 + 1/\tau_2 + \ldots$ in order to find the lifetime arising from all processes. This also applies to a real residual vacuum, where several atomic species are present.
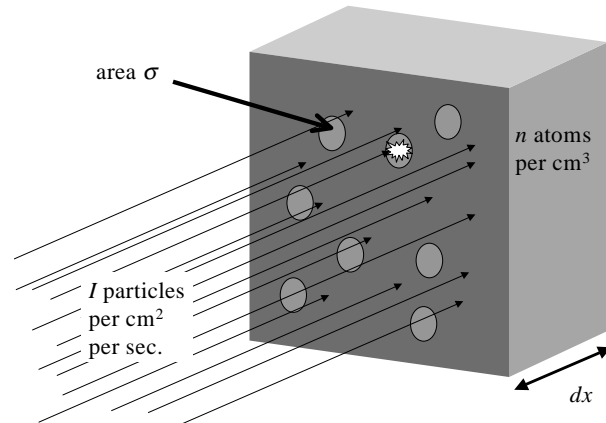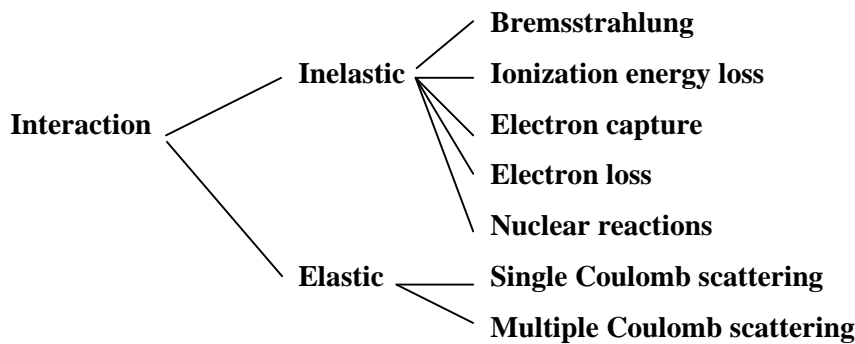
Fig. 1 Definition of cross section.

3. THE INTERACTION BETWEEN CHARGED PARTICLES AND RESIDUAL-GAS ATOMS

The interactions to be described subsequently depend in general on the type of projectile in question, and to some extent also on the residual-gas atom considered. The atomic number of the projectile will be designated Z_i and the charge state q, whereas the atomic number of the rest gas atoms is called Z_t. The interactions will be divided into elastic processes, where no energy transfer takes place, and inelastic processes, where energy is lost by the projectile. The processes can be further classified according to the following division:

Interaction
- **Inelastic**
  - **Bremsstrahlung**
  - **Ionization energy loss**
  - **Electron capture**
  - **Electron loss**
  - **Nuclear reactions**
- **Elastic**
  - **Single Coulomb scattering**
  - **Multiple Coulomb scattering**

Disregarding nuclear reactions and emission of bremsstrahlung, atomic collisions can be divided into two types, namely so-called electronic collisions and nuclear collisions. In the electronic collisions, the struck atoms are either excited or ionised. In the nuclear collisions, the interacting atoms recoil as a whole. The typical energy transfer is much larger for electronic than for nuclear collisions for projectile energies above a few keV. Hence, it is the electronic collisions that lead to the so-called ionisation energy loss; it is called the ionisation energy loss although atomic excitations also contribute. The nuclear collisions, on the other hand, lead to scattering of the beam particles. These scattering processes will be discussed in section 3.2 below.

3.1 Inelastic processes

The most important inelastic processes occurring when charged particles collide with residual-gas atoms will be described. In some special cases, ions may also interact with the black-body radiation emitted by the surrounding vacuum chambers. This interaction may lead to photo-ionisation of weakly bound negative ions [4]. This effect can only be reduced by cooling the vacuum chambers.

3.1.1 Bremsstrahlung by electrons and positrons

When charged particles are accelerated, they emit electromagnetic radiation, i.e. photons. This emission is only significant for light particles, and only has practical relevance for electrons (and positrons). In this respect electrons and positrons have the same radiation characteristics. When electrons and positrons penetrate matter, they are accelerated in the fields of the atomic nuclei, and electrons, and emit the so-called bremsstrahlung. This bremsstrahlung is very strong for relativistic electrons and the average energy loss due to bremsstrahlung is much larger than the ionisation energy loss to be described in the next subsection. Photons of all energies, only limited by the electrons kinetic energy E, can be emitted. The emission of bremsstrahlung is described by the so-called Bethe-Heitler cross section, differential in photon energy

$$\frac{d\sigma}{d\hbar\omega} = \frac{4}{3}\frac{1}{nL_0}\frac{1}{\hbar\omega}(1 - \frac{\hbar\omega}{E} + \frac{3}{4}(\frac{\hbar\omega}{E})^2)$$

where L_0 is the radiation length given by

$$\frac{1}{L_0} = 4Z_t^2\alpha n r_e^2 \ln(183 Z_t^{-1/3}).$$

Here $r_e = e^2/mc^2 = 2.82\cdot10^{-15}$ m is the classical electron radius, $\alpha = e^2/mc^2$ the fine structure constant and n the atomic density. In the above formula contributions from scattering off the atomic nuclei have been included but a small term resulting from scattering off the electrons of the residual gas atom has been neglected. This is usually well justified due to the Z_t^2 front factor in the Bethe-Heitler cross section. The radiation length for H_2 and CO_2 corresponds to 7523m and 183m, respectively, at atmospheric pressure. The behaviour of this Bethe-Heitler cross section is shown in Fig. 2.
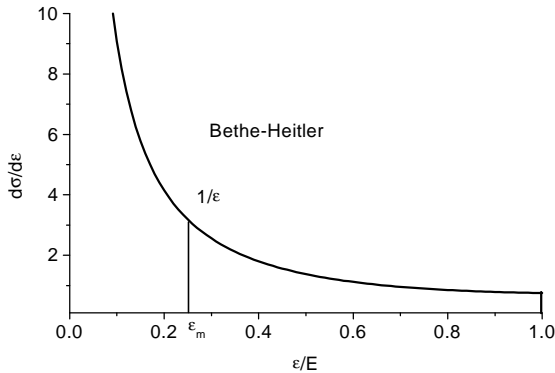
Fig. 2 Differential bremsstrahlung spectrum; the Bethe-Heitler spectrum.
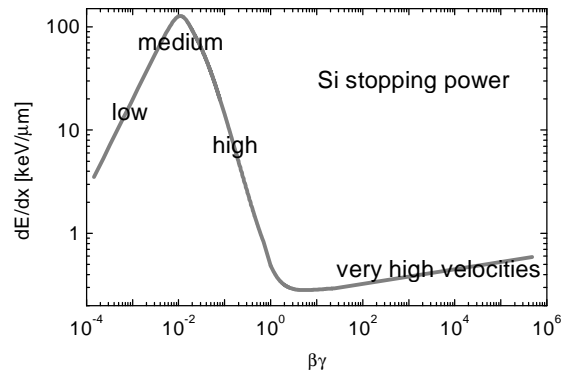
Fig. 3 Stopping power of silicon as a function of the relativistic $\beta\gamma$ factor.

When electrons are circulating in a storage ring they emit bremsstrahlung during the collisions with the residual-gas atoms, and if the photon energy is too large, the particle will be lost due to the finite momentum acceptance of the ring. This acceptance might be determined by the aperture of the vacuum chamber in a region of finite dispersion, or by the so-called dynamical aperture beyond which the transverse motion is unstable. Finally, the available RF voltage might determine the longitudinal acceptance. Hence the important cross section is the integral of the Bethe-Heitler cross section from the energy acceptance ε_m to the beam energy E

$$\sigma_{brems} = \int_{\varepsilon_m}^{E}\frac{d\sigma}{dE}dE \approx \frac{4}{3}\frac{1}{nX_0}\left[\ln\frac{E}{\varepsilon_m} - \frac{5}{8}\right].$$

This bremsstrahlung is usually the residual-gas effect determining the lifetime of an electron beam in a storage ring. The lifetime can now be calculated and expressed in units of the radiation length, but we give here the formula for the lifetime expressed directly only in terms of the target atomic number Z_t

$$\frac{1}{\tau_{brems}} = \frac{16 r_e^2 Z_t^2 nc}{411} \ln\left[\frac{183}{Z_t^{1/3}}\right]\left[\ln\frac{E}{\varepsilon_m} - \frac{5}{8}\right].$$

A very strong dependence on the target atomic number is observed, which means that even a small amount of a heavy gas may have a higher influence on the lifetime than the usually dominating hydrogen content.

3.1.2 Ionization energy loss

The ionisation energy loss is characterised by the so-called stopping power, the energy loss per unit distance. The velocity-dependence of the stopping power for singly-charged particles is given in Fig. 3. This figure shows the stopping power of silicon, which normally is not relevant for vacuum effects. The behaviour is, however, qualitatively, and also to a large extent quantitatively independent of atomic number. Clearly, the stopping power is proportional to atomic density. Actually, the figure shows the stopping power as function of $\beta\gamma$, which is the particle momentum divided by the rest mass. As usual, $\beta = v/c$ is the particle velocity relative to the velocity of light, and $\gamma = (1-\beta^2)^{-1/2}$. This quantity $\beta\gamma$ is a very convenient parameter, which equals β when $\beta\gamma \ll 1$ and γ when $\beta\gamma \gg 1$. For small velocities, the stopping power increases linearly with velocity until it reaches a maximum. This maximum occurs at a velocity corresponding to typical target electron velocities, where energy is easily transferred to the electrons. The corresponding proton energy is around 100 keV. Above the maximum, the stopping power decreases inversely proportional to the velocity squared, until a shallow minimum is reached at around $\beta\gamma \approx 1$. For even higher velocities, the stopping power has a logarithmic increase, the so-called relativistic rise. Above the maximum, the stopping power can be described by the famous Bethe-Bloch formula with corrections

$$-\frac{dE}{dx} = \frac{4\pi Z_i^2 Z_t e^4}{mv^2} n\left\{\ln\left(2mc^2\beta^2\gamma^2/I\right) - C/Z_t - \beta^2 - \delta/2\right\}.$$

The velocity dependence described above is directly seen from this formula. The parameter describing the atomic properties of the residual-gas atoms is the so-called mean ionisation potential I, which is given approximately by $I = Z_t \cdot 14$ eV. The shell-correction C/Z_t is usually a small correction taking into account that the atomic electrons have a finite velocity. The density effect δ is a relativistic correction saturating the distant atomic collisions at high values of $\beta\gamma$ due to polarisation of the atomic electrons. The Bethe-Bloch formula can be written in a form more suitable to estimate pressure-dependent ionisation energy-loss effects [3]

$$-\frac{dE}{dx} = K_{BB} P_t m_t Z_t q^2 \beta^{-2}\left\{11.1 - 0.9\ln Z_t + \ln(\beta^2\gamma^2)\right\}.$$

Here P_t is the pressure in mbar and m_t the number of atoms/molecule, and $K_{BB} = 0.0137$ eV/mbar/m.

In most cases, the ionisation energy loss is an unimportant effect masked by other effects. It can, however, be observed both for bare and almost bare nuclei at high energy [3]. Another aspect of the energy loss is that there is a spread, since it is formed by a series of discrete losses. Hence the average energy loss, and the width of the energy loss distribution, the so-called straggling, characterise the energy loss. The above two formulae describe the average energy loss. The energy-loss distribution is Gaussian at high velocities for not too thin targets.

3.1.3 Electron capture and loss

A positive ion can capture electrons from the residual-gas atoms during a collision. Similarly, a not fully stripped ion can loose an electron. Electron capture and loss effects cannot be described by one or a few simple formulae, since the cross section in general is a complicated function of the projectile charge Z_i, the projectile charge state q, the target atomic number Z_t and the projectile velocity β, $\sigma = \sigma(Z_i, q, \beta, Z_t)$.

The charge exchange processes can be divided according to the following scheme:

$$X^{q+} + Y \rightarrow X^{(q+1)+} + Y + e$$

$$X^- + Y \rightarrow X + Y + e$$

$$X^{q+} + Y \rightarrow X^{(q-1)+} + Y^+$$
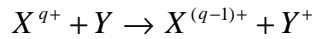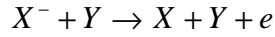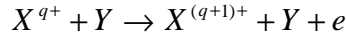
where the first two processes are electron loss by positive and negative particles, respectively, whereas the last process is electron capture. The projectile of charge q is here represented by X and the rest gas atom by Y. Clearly, multiple loss and capture processes are also possible, but they are in general much less probable than single processes.

Some scaling relations and qualitative features can, however, be given, but in general it can only be said that the relevant cross section should be found in the literature, either from measurements or from calculations. Measurements and calculations of charge exchange cross sections have been an important part of atomic physics for many decades, and the qualitative, and to a large extent also the quantitative, behaviour of the cross sections are understood today.

Qualitatively, electron-capture cross sections have a maximum at projectile velocities corresponding to the typical electron velocity of the target atom. This qualitative behaviour is given in Fig. 4. This can be easily be understood, since the captured electron has to follow the projectile, which then is the case before the collision for equivelocity particles. Similarly, for electron loss cross sections. From the same type of arguments, there exist for a given projectile with given velocity passing through a given material a so-called equilibrium charge, where the capture and loss cross sections are equal. Bohr has estimated this cross section [3] to be

$$\overline{q} \approx Z_i (1 - \exp(-\frac{\beta}{\alpha Z_i^{0.67}})) \, .$$

This equilibrium charge state only depends on the projectile velocity. From known cross sections for ions of this equilibrium charge state, the cross sections for other charge states can be estimated from simple scaling relations [3]

$$\sigma_c(q) \approx \sigma_c(\overline{q})(\tfrac{q}{\overline{q}})^a$$

$$\sigma_l(q) \approx \sigma_c(\overline{q})(\tfrac{q}{\overline{q}})^b$$

where $a \approx 4$ and $b \approx -2.3$ for charges lower than the equilibrium charge state and $a \approx 2$ and $b \approx -4$ for higher charge states. Many other scaling relations exist.
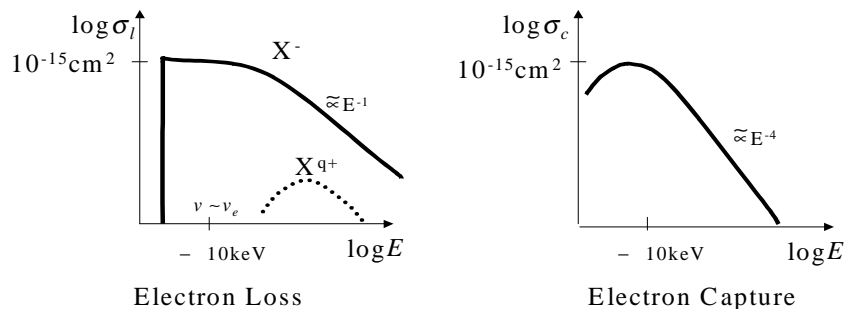

Fig. 4 Qualitative behaviour of electron loss and capture cross sections.

As an important example for a negative ion, we show in Fig. 5 the electron loss cross section for H$^-$ ions on H$_2$ molecules [5]. The cross section is seen to have a shallow maximum of around 10^{-15} cm^2 at around 100 keV, and to decrease slowly with increasing energy, slightly faster than E^1.

The electron capture cross section for protons, H$^+$, colliding with H$_2$ molecules is shown in Fig. 6 [5]. Again a maximum, with a value of around 10^{-15} cm^2, is observed, but with a rather fast decrease towards both lower and higher energies. The decrease for high energies is indeed very fast, roughly proportional to energy to the eighth power, E^8.
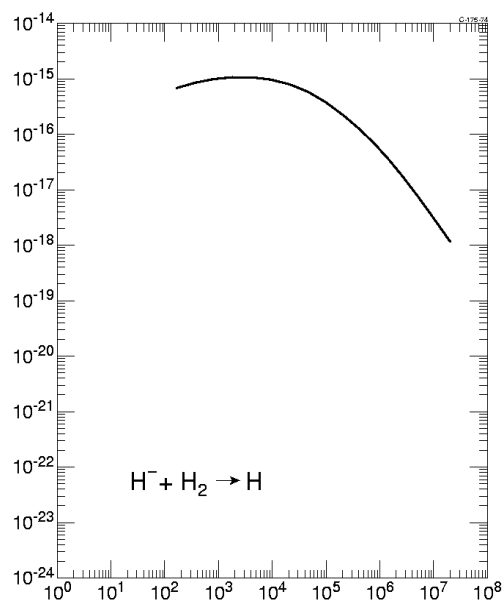

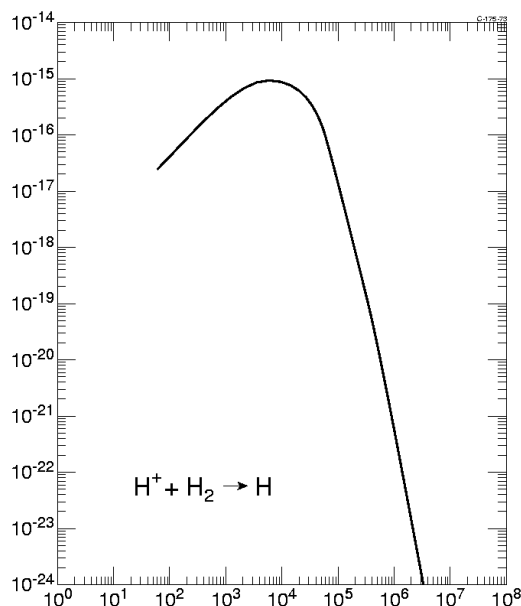Fig. 5 Electron loss cross section for H$^-$ on H$_2$ as function of energy.

Fig 6. Electron capture cross section for H$^+$ on H$_2$ as function of energy.

Finally, as an example of an electron capture cross section for highly charged ions, we show in Fig. 7 the capture cross section as function of energy for highly charged ions colliding with argon [6]. The scaling implied by the choice of axes is observed to apply reasonably well. The decrease with energy is roughly with E^4. Note, that the displayed cross sections are normalised to the charge state q, which means that electron capture cross sections for highly charged ions can be much larger than the geometrical cross sections.
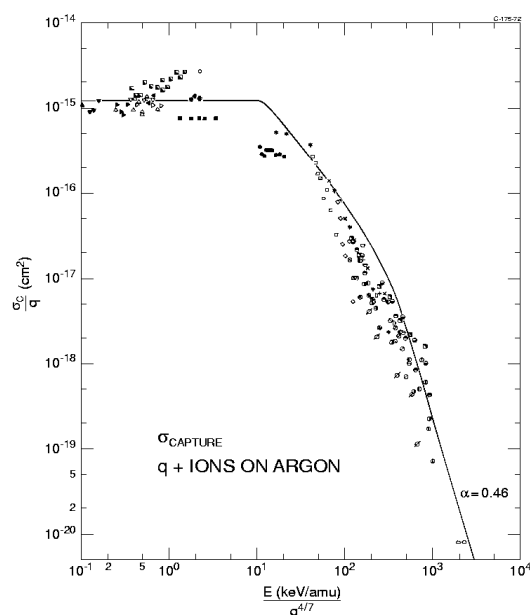

Fig. 7 Electron-capture cross section for highly-charged ions colliding with Ar atoms.

3.1.4 Nuclear reactions

The cross section for nuclear reactions is in general much smaller than atomic cross sections, as was also seen from the comparison between the geometrical cross sections above. There are, however, cases where a nuclear process is the dominating loss process. For example for bare nuclei at high energy, capture cross sections are very small; see above. Another important case is antiprotons, where electron capture clearly is excluded. Furthermore the energy should be so high that the elastic processes described below can be neglected.

In general, the relevant nuclear cross section has to be looked up in the literature. Some of the relevant cross sections for elementary particles can be found in [7]. The geometrical estimate of a nuclear cross section made in section 2 of around 10^{-24} cm^2 gives reasonable estimates for protons colliding with protons at beam momenta of around 100 MeV/c. At relativistic energies, above 1 GeV/c, the cross section is around a factor of 100 smaller.

3.2   Elastic processes

In the beginning of section 3 it was argued that the so-called nuclear collisions, where the residual-gas atom recoils as a whole, are almost elastic; i.e. there is only a very small energy transfer. There is, however, a significant scattering of the projectile associated with these collisions. If the projectile in a single-collision event is scattered outside the ring acceptance, it will be lost and lead to a reduction in the lifetime. The ring acceptance can either be physical, determined by the transverse aperture of the vacuum chambers, or it can be dynamical, determined by the boundary between stable and unstable motion. Additionally, multiple or plural scattering can lead to an increase of the beam emittance. The emittance growth can clearly be so large and fast that particles again are lost on the apertures, but a dilution of the density in phase space is in general disturbing. A slow multiple scattering can, however, be counteracted by phase-space cooling, e.g. electron or stochastic cooling or in the case of electrons by radiation damping.

3.2.1 Single scattering

The scattering between point-like charged particles is described by the so-called Rutherford cross section, which in the small-angle approximation reads

$$\frac{d\sigma}{d\Omega} = \left(\frac{2Z_t Z_i e^2}{m_0 c^2 \beta^2 \gamma} \right)^2 \frac{1}{\theta^4}$$

Deviations from this very simple formula exist for small angles due to electronic screening effects of the atomic nucleus and for large angles due to the finite size of the nucleus; see Fig. 8.
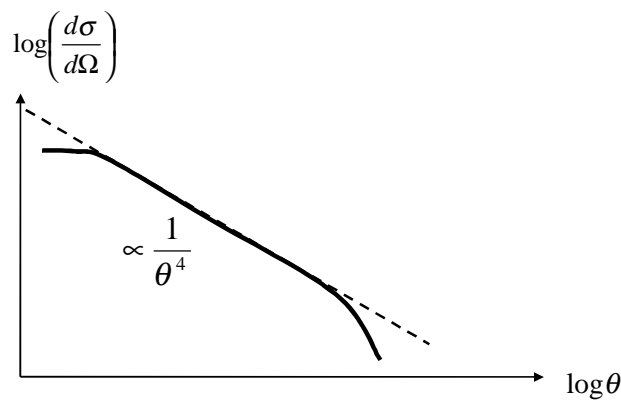

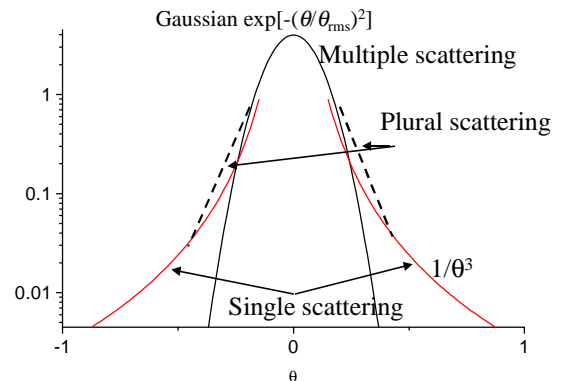Fig. 8 Qualitative behaviour of the Rutherford scattering cross section.

Fig. 9 Angular scattering distribution.

The relevant cross section for calculation of lifetimes is the integral of this Rutherford cross section from θ_0, the minimum angle for which loss occurs, to a very large angle. This maximum angle need not be specified since the most important contribution comes from the small angles. The resulting cross section is

$$\sigma = \int_{\theta_0}^{\theta_{max}} \frac{d\sigma}{d\Omega} d\Omega = \frac{2r_p^2 (Z_i / A)^2 Z_t^2 \pi}{\beta^3 \gamma^2 \theta_0^2}$$

where $r_p = 1.546 \cdot 10^{-18}$ m is the classical proton radius. For electrons the projectile mass in amu is $A = 1/1836$, which means that the formula can be written in terms of the classical electron $r_e = 2.82 \cdot 10^{-15}$m.

The minimum aperture gives the maximum acceptable scattering angle, and in the case of one small aperture b with a betatron amplitude at this position of β_u, the angle is given by

$$\theta_0 = \frac{b}{\sqrt{\beta_u \overline{\beta}}}$$

where the betatron function β is averaged over the whole circumference. In the case of a modern synchrotron radiation source, this aperture would be the height of the undulator vacuum chamber with smallest gap.

3.2.2 Multiple scattering

Many small-angle scattering events will lead to an increase of the emittance of a beam. Since this can be a relatively slow process, cooling the beam with a suitable cooling method, e.g. electron cooling or stochastic cooling can compensate it. The multiple scattering in a given thickness of material s is given by

where p is the momentum of the projectiles and again L_0 the radiation length. In a storage ring, a more

$$\sqrt{<\theta^2>} = \theta_{rms} = 14 \text{mrad} Z_i \sqrt{s/L_0} / p[\text{GeV/c}]$$

interesting quantity is the emittance increase per unit time, which can be expressed by the increase in the divergence by

The increase in divergence is related to the radiation length by

$$\frac{d\varepsilon}{dt} \cong 4 < \beta_{H,V} > \frac{d<\theta^2>}{dt}.$$

From this expression, one can calculate for example the time it takes for the emittance to grow from

$$\frac{d<\theta^2>}{dt} = 2.6 \cdot 10^{-4} \frac{c}{X_0} \frac{1}{\beta^3 \gamma^2} \left(\frac{Z_i}{A_i} \right)^2 .$$

an initial to a final value

In general, there is clearly a transition between single Coulomb scattering and multiple scattering.

$$\Delta t = \frac{\varepsilon_{final} - \varepsilon_{init}}{4 < \beta_{H,V} > (d<\theta^2>/dt)}.$$

This so-called plural scattering occurs in the transition region, and the qualitative behaviour of the scattering angle distribution is given in Fig. 9.

4.   LOCAL VERSUS AVERAGE PRESSURE

The average pressure determines in general the lifetime of a beam, and the emittance growth. There are however, exceptions to this. For example if there is a local pressure bump, the aperture determining the single-scattering lifetime calculated in subsection 3.2.1 is the aperture $(1/4+m/2)\lambda$ downstream of the pressure bump. Here λ is the betatron wavelength and m an integer. This is because a scattering will initiate a betatron oscillation, which has a maximum amplitude at these distances downstream of the scattering position.

The other important issue concerning high local pressures is the background stemming from collisions between the beam particles and the residual gas. This background can, for example, be the background in a detector in a collider, it can be the high-energy γ-radiation emerging from a straight section in a synchrotron-radiation source, or it can be the neutralised ions giving a background in a capture-experiment in a cooler synchrotron. And there are inevitably other examples, where special care has to be taken in order to minimise local pressure bumps.

5.   CONCLUSIONS

In the present contribution to the CERN Accelerator School on Vacuum Technology the different vacuum-related processes leading to a degradation of the accelerator performance have been described. The dominating processes for different particles at different energies are outlined in Fig. 10. In several cases, the lifetimes can be estimated from the description presented, but in many cases the literature has to be consulted in order to find the relevant cross sections.
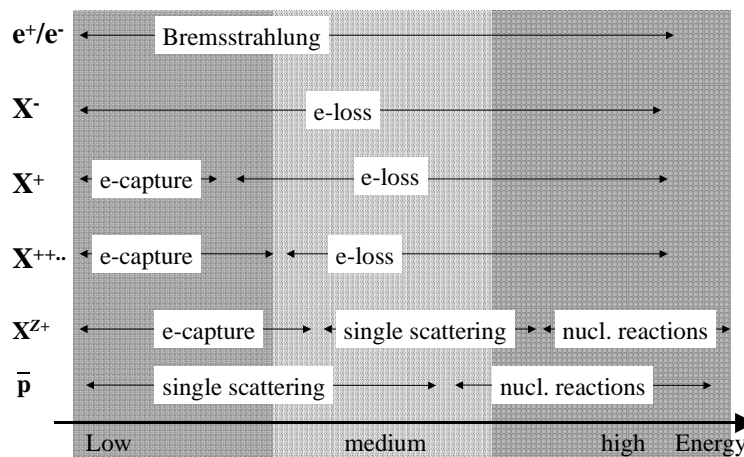

Fig. 10 The most important residual gas interactions for different projectile types in the different energy regimes.

REFERENCES

[1] A. Wrulich, Single-beam lifetime, CERN Accelerator School, Fifth General Accelerator Physics Course, CERN 94-01, p. 409

[2] C. Bochettta, Lifetime and beam quality, CERN Accelerator School, Synchrotron Radiation and Free Electron Lasers, CERN 98-04, p. 221.

[3] B. Franzke, Interaction of stored ion beams with the residual gas, CERN Accelerator School, Fourth Advanced Accelerator Physics Course, CERN 92-01, p. 100

[4] H.K. Haugen, L.H. Andersen, T. Andersen, P. Balling, N. Hertel, P. Hvelplund, and S.P. Møller, Phys . Rev. A **46** (1992) R1.

[5] Data on collisions of hydrogen atoms and ions with atoms and molecules (I), JAERI-M, 83-013, Japan Atomic Energy Research Institute, 1983.

[6] H. Knudsen, H.K. Haugen, and P. Hvelplund, Phys. Rev. A **23** (1981) 597.

[7] R.M. Barnett, Review of Particle Physics, Phys. Rev. D **54**,1 (1996).